Dynamic design considerations for offshore wind turbine jackets supported on multiple foundations

Saleh Jalbi[1,2], Georgios Nikitas[1], Subhamoy Bhattacharya[1], and Nicholas Alexander[3]

[1]University of Surrey, Guildford, United Kingdom
[2]Robert Bird Group, London, United Kingdom
[3]University of Bristol, Bristol, United Kingdom

Corresponding Author:
Professor Subhamoy Bhattacharya
Chair in Geomechanics
University of Surrey
United Kingdom
Email: S.Bhattacharya@surrey.ac.uk

Abstract

To support large wind turbines in deeper waters (30-60 m) jacket structures are currently being considered. As offshore wind turbines (OWT's) are effectively a slender tower carrying a heavy rotating mass subjected to cyclic/dynamic loads, dynamic performance plays an important role in the overall design of the system. Dynamic performance dictates at least two limit states: Fatigue Limit State (FLS) and overall deformation in the Serviceability Limit State (SLS). It has been observed through scaled model tests that the first eigen frequency of vibration for OWTs supported on multiple shallow foundations (such as jackets on 3 or 4 suction caissons) corresponds to low frequency rocking modes of vibration. In the absence of adequate damping, if the forcing frequency of the rotor (so called 1P) is in close proximity to the natural frequency of the system, resonance may occur affecting the fatigue design life. A similar phenomenon commonly known as "*ground resonance*" is widely observed in helicopters (without dampers) where the rotor frequency can be very close to the overall frequency causing the helicopter to a possible collapse. This paper suggests that designers need to optimise the configuration of the jacket and choose the vertical stiffness of the foundation such that rocking modes of vibration are prevented. It is advisable to steer the jacket solution towards sway-bending mode as the first mode of vibration. Analytical solutions are developed to predict the eigen frequencies of jacket supported offshore wind turbines and validated using the finite element method. Effectively, two parameters govern the rocking frequency of a jacket: (a) ratio of super structure stiffness (essentially lateral stiffness of the tower and the jacket) to vertical stiffness of the foundation; (b) aspect ratio (ratio of base dimension to the tower dimension) of the jacket. A practical example considering a jacket supporting a 5MW turbine is considered to demonstrate the calculation procedure which can allow a designer to choose a foundation. It is anticipated that the results will have an impact in choosing foundations for jackets.

Keyword: Offshore Wind Turbines, Jacket Structures, Natural Frequency, Rocking Mode of Vibration, Sway-Bending Mode of Vibration, Multiple Foundations.

1.0 Introduction

1.1 Wind turbines supported on monopiles and jacket on piles/suction caissons

Jackets or seabed frames supported on multiple shallow foundations are currently being installed to support offshore wind turbines in deep waters ranging between 23 m and 60 m, see for example Borkum Riffgrund 1 (Germany, water depth 23 to 29 m), Alpha Ventus Offshore (Germany, water depth 28 to 30 m), Aberdeen Offshore wind farm (Scotland, water depth 20 to 30m) (4C Offshore Limited [1],[2]). The jackets are typically designed as three or four legged and are supported on either deep foundations (piles) or shallow foundations (suction caissons). The height of the jacket currently in use is between 30 and 35 meters and is governed by water depth above mudline and wave height (50 year return period) following the guidance of DNV-OS-J101 (2014). However, it is expected that future offshore developments will see jacket heights up to 65 m to support larger turbines (12MW to 20MW) in deeper waters. Figure 1 shows a schematic of a 3-legged jacket inspired by some recent offshore developments.

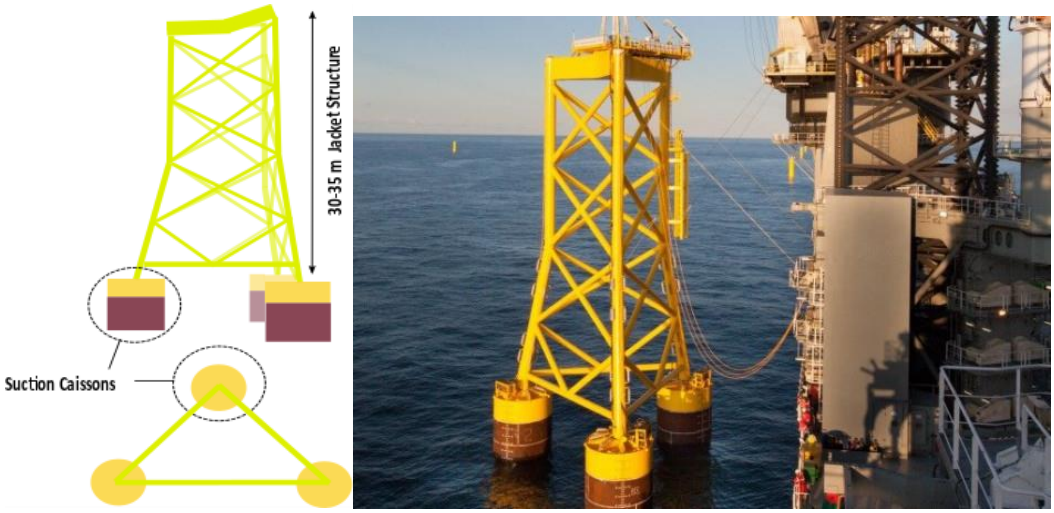

Figure 1: Schematic of a 3-legged jacket supported on a suction caisson

There are obvious differences between the behaviour of jacket supported wind turbines and monopile supported ones as illustrated through Figures 2, 3 and 4. The difference can be classified into two distinct types:

(a) For monopile supported wind turbine, the overturning moment resulting from the wind and the wave is transferred to the supporting ground through moment and the monopile acts as a moment resisting foundation. On the other hand, for a jacket, the overturning moment is transferred through axial push-pull (in combination with the lateral base shear to maintain lateral equilibrium), see Figure 2 for a schematic diagram.

(b) The modes of vibration for monopile supported wind turbines or for that matter any foundation supported on piles will be sway bending as the foundation is very stiff compared to the tower, see Figure 3. For the corresponding jacket supported wind turbines on shallow foundation, the first modes of vibration is most likely to be rocking due to the relatively lower vertical stiffness of shallow foundations as shown in Figure 4. Further details on different types of modes of vibrations are discussed in [8,9,10].

One of the aims of this paper is to highlight the importance of avoiding rocking type vibration for wind turbine support structure by learning lessons from an equivalent problem from aerospace industry – the "*helicopter ground resonance*". OWT jackets supported on shallow foundations are a new

innovation which lack a track record of dynamic and long-term performance. For this reason, it is important to learn lessons from dynamically similar types of engineering problems and of close similarity is ground resonance in helicopters. It is therefore considered useful to study the problem.

The other aims and the scope of this paper are as follows:

(a) Develop and validate analytical solution to study the vibration of offshore wind turbine jackets supported on shallow gravity based foundations and piled foundations.

(b) To find out the mechanics of the problem based on non-dimensional groups that can characterise the different vibration modes of the system and identify the controlling parameters affecting the vibration modes.

(c) To provide insights for enhanced dynamic performance and develop simple design rules.

(d) To demonstrate the practical implications by taking an example and show the calculation procedure.

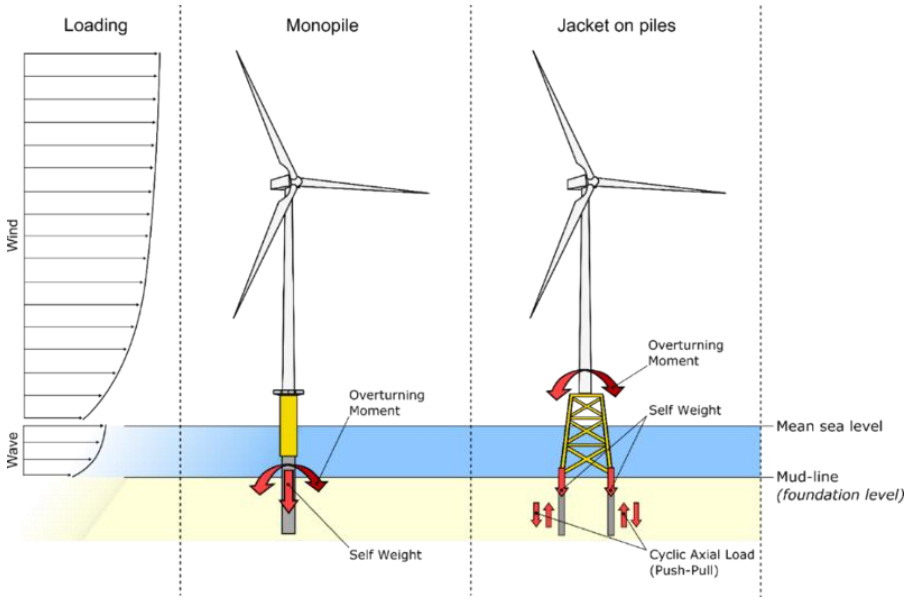

Figure 2: Schematic of a load transfer for two types of foundation system. *Note: The aim of figure is to shows how the overturning moment is resisted. To maintain equilibrium, both types of foundation will have a lateral resistance component at the mudline*

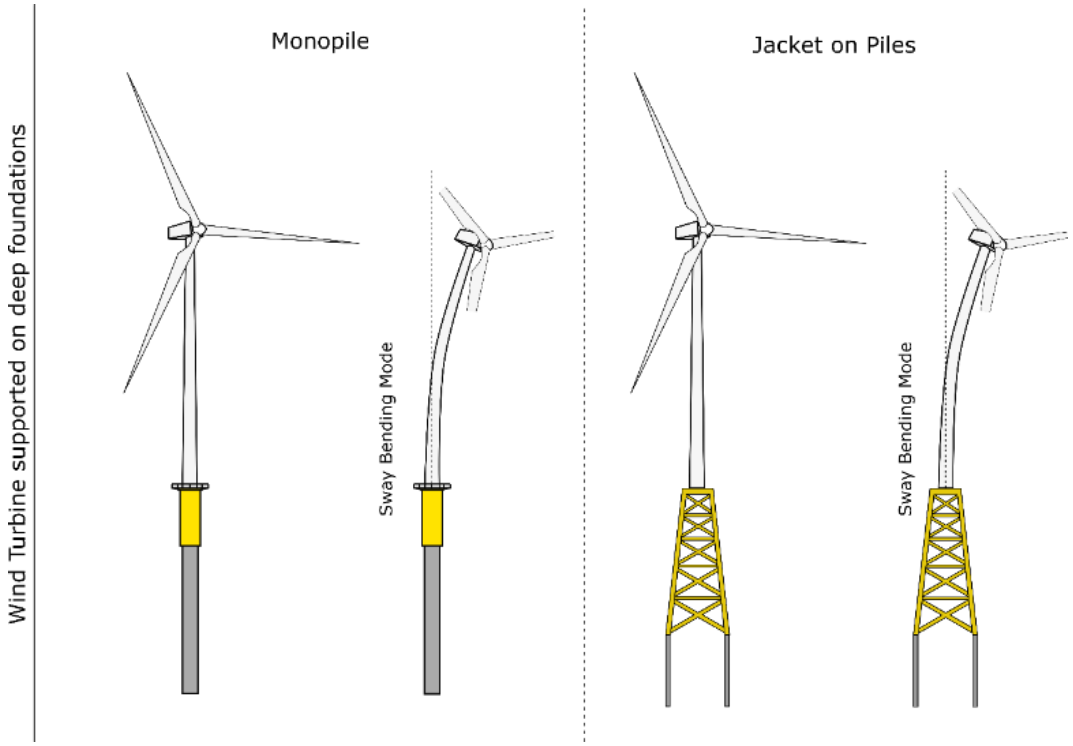

Figure 3: Sway-Bending Mode of Vibration for pile supported wind turbines. It may be noted that the foundation is very stiff vertically

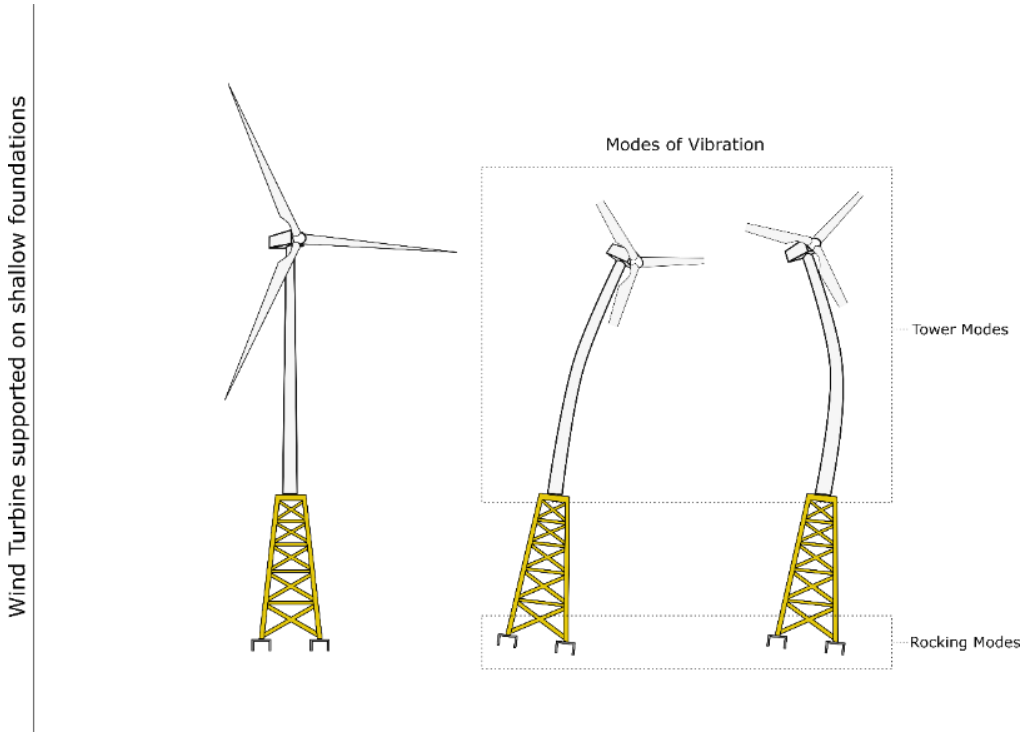

Figure 4: Rocking Mode of Vibrations

2.0 Ground Resonance of helicopter & OWT structure supported on shallow foundation

Figure 5 shows still photographs from the well-known helicopter resonance problem known as ground resonance, the video can be accessed in [13]. Effectively, due to the imbalance in the helicopter rotor the RPM (Revolutions Per Minute) induced oscillations get in phase with the rocking frequency of the helicopter on its landing gears. This leads to collapse and the experiment is schematically shown in Figure 6. The helicopter starts rocking about the two landing pads (skids) until the stresses induced through resonance exceed the strength of the materials and connections causing failure. There are many similarities between these two systems: *both are essentially a structural beam carrying a heavy rotating mass resting on multiple supports*, see Figure 7.

Mathematically, the mass and the stiffness matrices in a dynamic formulation will be similar. The structures in both systems will rock and there is considerable amount of energy in these modes of vibration. However, the difference is the plane of rotation of the rotors and the rotor speed. It may be noted that the resonance phenomenon to be studied is irrespective of the planes of rotation. The objective in this study is to learn from other engineering disciplines given that wind turbines jackets supported on suction caissons are new structures *with no track record*. As the motion under consideration is rocking, the vertical stiffness of the supports is a governing parameter. For a jacket structure, at the onset the vertical stiffness may not be identical and therefore they are shown as K_1 and K_2. It is clear that resonance must be avoided and this emphasizes the importance of understanding the subtle aspects of the dynamic behaviour of jacket supported wind turbines only in relation to FLS (Fatigue Limit State) and SLS (Serviceability Limit State) but also from the point of view of monitoring and O & M (Operation and Maintenance).

Moreover, it is interesting to note how the target frequency in the soft-stiff frequency is shifting with turbine size. For instance, a Vestas 8MW OWT has a soft-stiff frequency band of 0.2-0.24 Hz which is very close to the predominant North sea frequency of 0.1 Hz. This is even more challenging for Chinese wind farms as the predominant wave frequency for Bohai and Yellow sea is 0.2 Hz. Thus, even though the amplitude of the 1P and 3P excitations are relatively low, wave loads (which is also have a close forcing frequency) have a considerably higher energy content. This higher energy content in combination with a low vertical stiffness will induce a rocking type vibration, and though this rocking might not have ultimate failure effects as in the case of the helicopter, it may have further implications on the fatigue performance of the structure and opens the door to further research needed in this area where the considerations of the correct energy content of the loads and the incorporation of damping.

The dynamic performance of jacket supported OWTs incorporating Soil Structure Interaction (SSI) is an area of active research [14-16]. The dynamic response of jackets under the action of waves of different periods and energy is studied by [14] using Finite Element analysis where the dynamic amplification factors (DAFs) are evaluated. The study shows that depending on the wave amplitude and period, the DAF may reach values of 1.2-1.3 which is significant given the magnitude of wave loads. Studies by [22] also modelled OWT jackets on a fixed base and assessed the fatigue damage on different types of welded joints. It was concluded that the interaction of both wind and wave loads have to considered when assessing the fatigue damage with wind loads providing the dominant contribution to the cumulative damage. Moreover, numerical studies by [15] show the importance of incorporating the flexibility of foundation in understanding the modes of vibration of the system when predicting the structural response. The SSI effect was introduced through distributed springs along the depth of the foundation. Similarly, [16] studied the effect of non-linearity of the ground profiles

in loose sands, medium sands and dense sands and concluded that the effect of SSI becomes predominant in looser sands. Other work by [19] showed, through numerical analysis, that incorporating SSI effects alters the natural frequency and the dynamic response of the leg and bracing members. Moreover, the study also showed that incorporating pile group effects has a noticeable effect on the fatigue analysis of the structure. The literature above builds upon previous work on SSI effects on jackets supporting oil and gas decks/platforms where [20] also performed a numerical study on a jacket supported on piles and showed that SSI reduces the natural period with an emphasis on the effect of the top soil layers on the frequency and [21] performed a scaled model tests showing the importance of SSI in predicting the response of offshore jackets to random loads.

Rocking type modes of vibration has been observed in small scale tests for jacket/seabed frame supported on shallow foundations, see reference [8, 10]. For offshore wind turbines, rocking modes can be quite complex where the vertical motion of the foundation interacts with the flexible bending modes of the tower together with the 1P rotor frequency and 2P/3P blade passing frequency. In some cases, depending on the stiffness and mass distribution of the superstructure (jacket and the tower with the huge RNA mass), the superstructure may or may not be in phase with the rocking motion of the foundations [9]. Furthermore, rocking modes of vibration will have a lower frequency which may be close to the wave frequency given the wave will have a higher energy of excitation. It is therefore advisable to avoid rocking modes for jacket supported shallow foundations. Judging from the literature above, a better understanding of the modes of vibration of the system is crucial for the dynamic analysis and assessing the fatigue life of the structure. The next section of the paper derives an analytical expression for rocking modes of vibration for OWT jacket supported on shallow foundations.

Figure 5: Ground Resonance of a helicopter

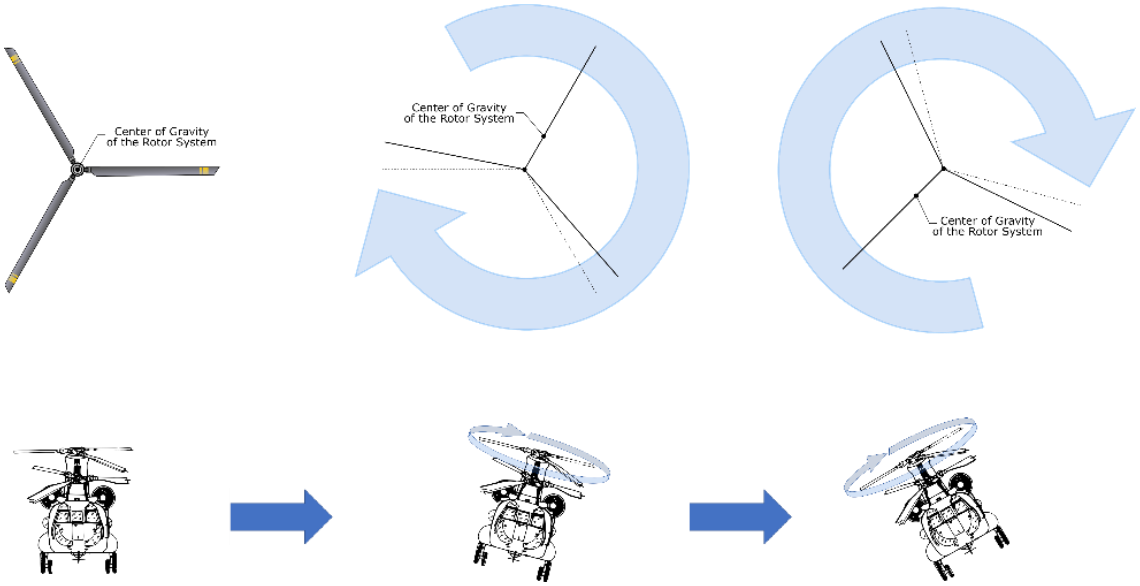

Figure 6: Rocking motion of a helicopter getting tuned with the RPM of helicopter rotor

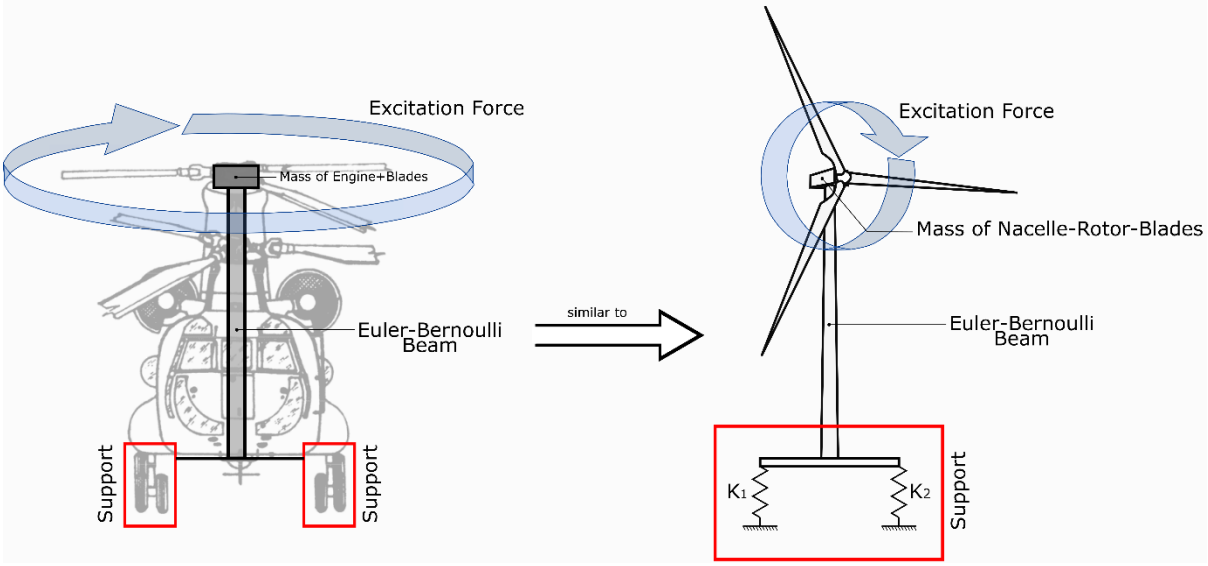

Figure 7: Similarities between a helicopter and Offshore wind turbine

3.0 Analytical solution for rocking modes of vibration for OWT jacket supported on shallow foundations

3.1 Simplified mechanical representation of the vibrating system

Figure 8 shows an idealisation of the vibration problem in hand i.e. eigen values of jacket supported on multiple foundations following the work of [10, 18]. The vibration of such a complex system is a 3D problem where oscillations may occur over multiple coupled planes depending on the locations of the centre of mass and centre of stiffness of the foundations. Under certain circumstances, a 3D problem can be simplified into a 2D, where vibrations in orthogonal planes may be uncoupled and studied

separately. This is generally true if the centre of mass of the foundation coincides with centre of stiffness and can be applied for different foundation arrangements. Examples of different foundation configurations in relation to the centre of mass and centre of stiffness are shown in Appendix 1. The foundation will vibrate in two principle axes i.e. highest variance of moment of inertia. The foundation can be modelled as two springs connected by a rigid base with a lumped mass m_1, whilst the superstructure (the jacket and wind turbine tower) can be modelled as an equivalent beam with a lumped mass at the tip. In the analysis, m_2 represents the mass of the Rotor-Nacelle Assembly (RNA) together with the total structural mass of the tower and the jacket and as shown is lumped at the tower tip. In this paper, m_2 has been computed using a FE package. However a detailed example on the methods of calculation for m_2 (i.e. how to lump it to the tower tip) and k_t using simple spreadsheet programs is provided in reference [17] and summarized in Appendix 2. Furthermore, guidance on the computation of the vertical stiffness of shallow caissons is provided in Appendix 3. This two-dimensional (2D) mechanical model can be applied to both three legged or four legged jackets as shown in Figure 9 to 12. For four legged jackets, vibration can occur at X-X' or Y-Y' planes as shown in Figures 9 and 10. It may be noted that a four-legged jacket on shallow foundations may vibrate in diagonal plane of conventional orthogonal plane. Similarly, for three legged jackets the rocking vibration modes will have three axes of symmetry as shown in Figures 8 and 9. Further discussion and the impact of three axes of symmetry on dynamic soil-structure interaction can be found in [9].

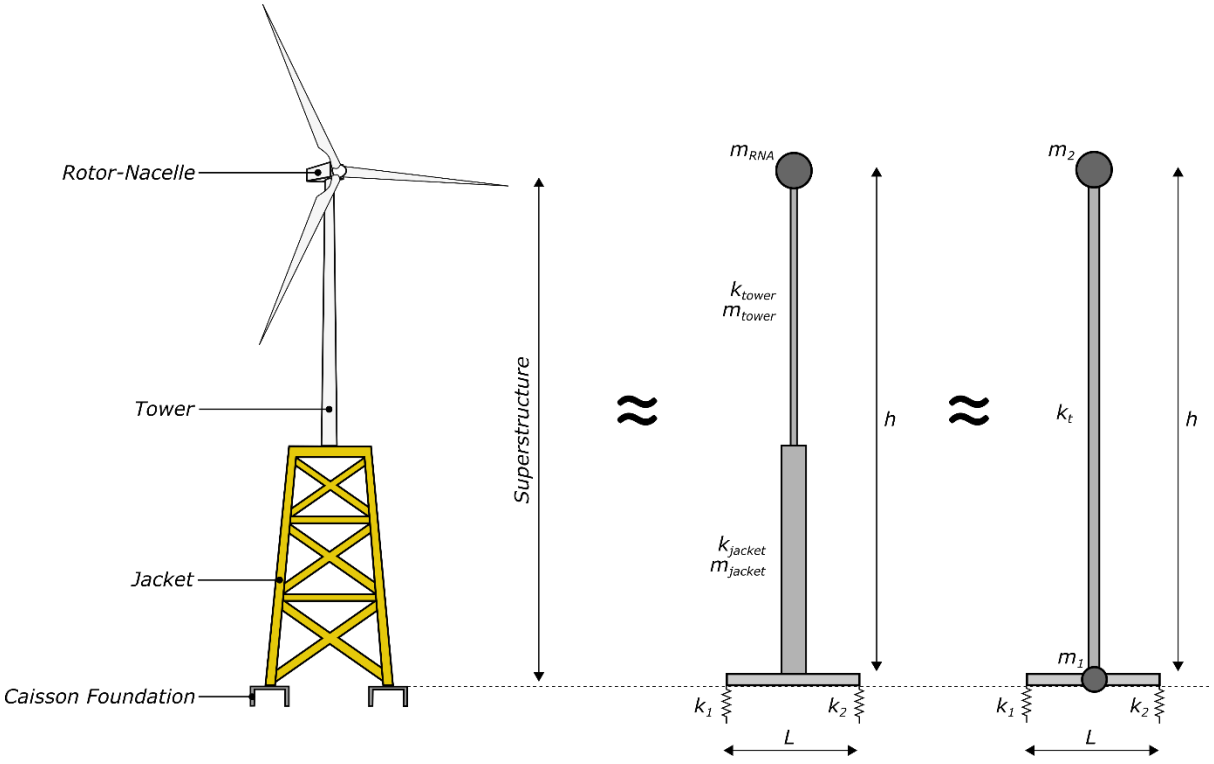

Figure 8: Mechanical Representation of jacket supported offshore wind turbines

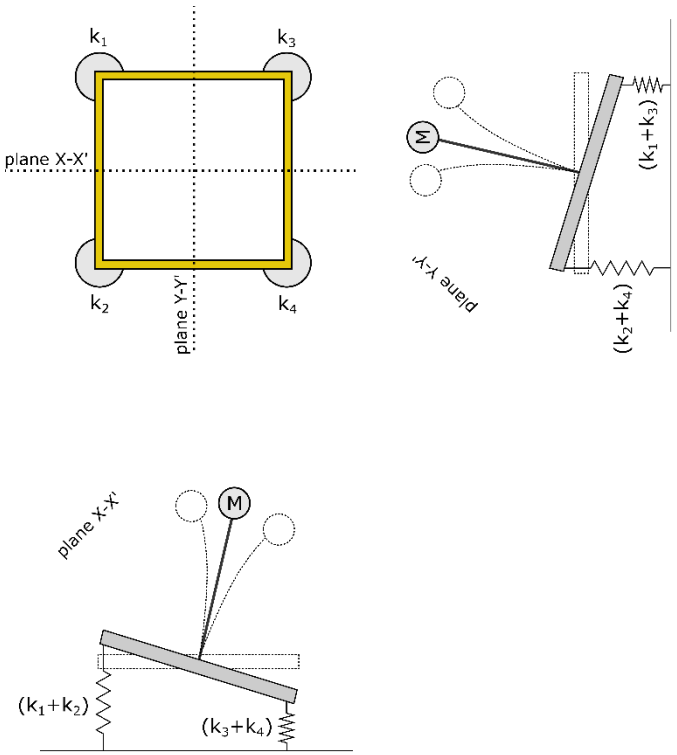

Figure 9: Rocking modes for four legged jackets about X-X’ and Y-Y’ planes

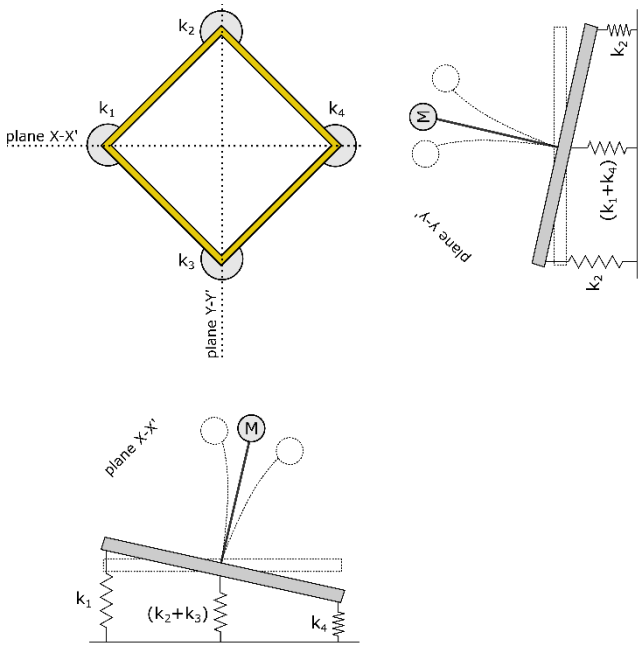

Figure 10: Rocking modes about diagonal planes

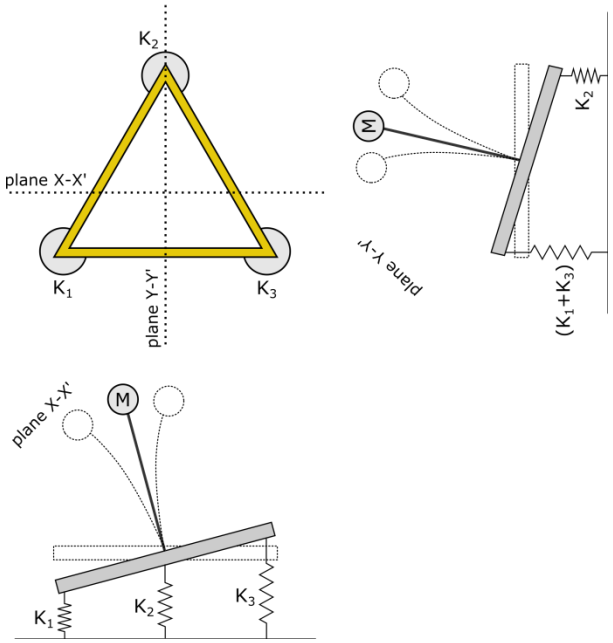

Figure 11: Rocking modes for three legged jackets

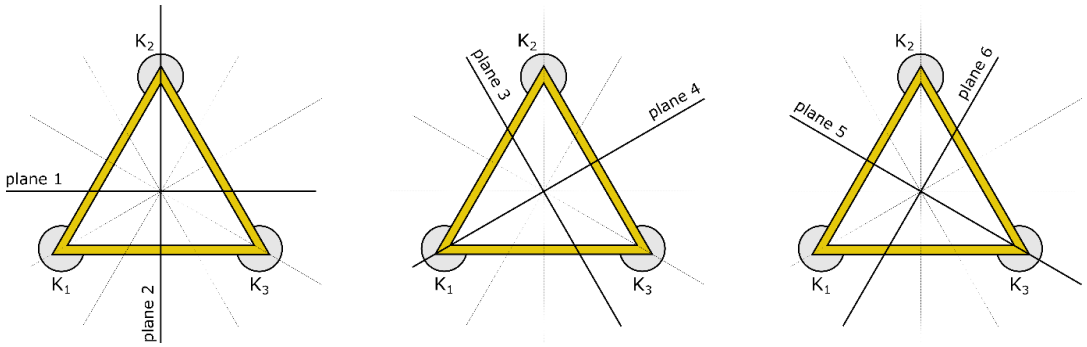

Figure 12: Planes of Symmetry

It may be noted that this method assumes the presence of translational restraints in the lateral direction at foundation level and only the vertical stiffness is considered due to the load transfer mechanism. Typically, the inherent lateral stiffness of the foundation will be sufficient, and the value of the vertical stiffness will govern the first natural frequency as shown in [17] by the authors. It was found in [17] that the idealization of the foundations (used in this paper) provides a close match with literature that utilized p-y and t-z springs for the foundations. In practice, one requires to carry out a refined analysis and this can be modelled by adding lateral springs (K_L) in addition to the vertical springs (k_1 and k_2). Thus, after the selection of a certain foundation size using the proposed simplified method (which only includes vertical springs) designers are encouraged to further refine structural models to include the lateral stiffness at the foundation level rather than a lateral restraint.

3.2 Mathematical derivation of the mass and stiffness matrices

The mass and stiffness matrices were assembled using Euler Lagrange's equations of potential and kinetic energy following the work of [3,4,5,6,7]. The allowable degrees of freedom are the movement of the rigid base, the rotation of the rigid base, and the bending of the tower as shown in Figure 13. u_1 and u_2 represent the vertical translations of the springs, u_g represents the translation of the centre of mass of the base m_1. u_T is the total translation of the tower and composed of two components: (a) the translation of m_2 due to rocking (where the tower is assumed to be rigid and does not bend) which

can be simply computed as htanΘ; (b) u_3 which is the translation due to bending of the tower. Figure 13 is a schematic showing the mass terms, the stiffness terms, and the degrees of freedom for a square base jacket.

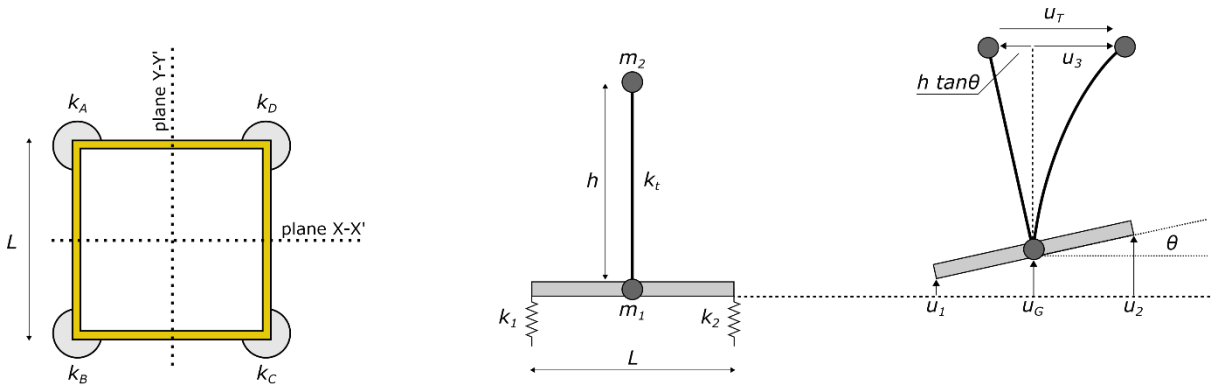

Figure 13: (a): Plan view of the foundation (b) stiffness and mass idealization of the system (c) degrees of freedom of the system

For the jacket vibrating about X-X' and Y-Y' axes, k_1 and k_2 can be computed using equations 1 to 4.

$$k_1 = k_A + k_B \qquad (1)$$

$$k_2 = k_C + k_D \qquad (2)$$

For vibrating abut Y-Y'

$$k_1 = k_A + k_D \qquad (3)$$

$$k_2 = k_B + k_C \qquad (4)$$

Using kinematic equations 5 and 6, the end displacements of the base (u_1 and u_2) are related to the small angle of rotation Θ. Equation 7 links the displacement of the tip of the tower with the movement of the base. It may be noted that there are relative movements between rocking and pure bending.

$$u_G = \frac{u_1 + u_2}{2} \qquad (5)$$

$$\theta = \frac{u_2 - u_1}{L} \qquad (6)$$

$$u_T = u_3 - h\tan\theta \qquad (7)$$

For small angle rotations $\tan\theta \approx \theta$

$$u_T \approx u_3 - \frac{h}{L}(u_2 - u_1)$$

As per equation Lagrange's equation is as follows

$$\frac{d}{dt}\frac{\partial T}{\partial \dot{q}_i}-\frac{\partial T}{\partial q_i}+\frac{\partial U}{\partial q_i}=\left(p_i\right) \qquad i=1,2,3 \qquad (8)$$

Where $q_1 \to u_1$ and $q_2 \to u_2$

Since the objective is to find the natural frequency of the system under free vibration, no external forces are applied on all degrees of freedom

Since the objective is to find the natural frequency of the system under free vibration, no external forces are applied

$$\left(p_1\right)=\left(p_2\right)=\left(p_3\right)=0$$

The Kinetic Energy of the System T is given by three components as shown by equation 9. The kinetic energy due to the translational acceleration of m_1 (rigid base), the kinetic energy due to the angular acceleration of the rigid base, and the translation acceleration of the lumped mass m_2 in the lateral and vertical directions (u_T and u_G respectively)

$$T=\frac{1}{2}m_1\dot{u}_G{}^2+\frac{1}{2}I_G\dot{\theta}^2+\frac{1}{2}m_2\dot{u}_T{}^2+\frac{1}{2}m_2\dot{u}_G{}^2 \qquad (9)$$

Where I_G is the moment of inertia of the rigid base

Which can be further simplified to:

$$T=\frac{1}{2}\left(m_1+m_2\right)\left(\frac{\dot{u}_1+\dot{u}_2}{2}\right)^2+\frac{1}{2}\left(\frac{1}{12}m_1L^2\right)\left(\frac{\dot{u}_2-\dot{u}_1}{L}\right)^2+\frac{1}{2}m_2\left(u_3-\frac{h}{L}\left(\dot{u}_2-\dot{u}_1\right)\right)^2$$

Further Algebraic simplification:

$$T=\frac{1}{8}\left(m_1+m_2\right)\left(\dot{u}_1{}^2+2\dot{u}_1\dot{u}_2+\dot{u}_2{}^2\right)+\frac{1}{24}m_1\left(\dot{u}_1{}^2-2\dot{u}_1\dot{u}_2+\dot{u}_2{}^2\right)+\frac{1}{2}m_2\left(\dot{u}_3{}^2-\frac{2h}{L}\left(\dot{u}_3\dot{u}_2-\dot{u}_3\dot{u}_1\right)+\frac{h}{L^2}{}^2\left(\dot{u}_1{}^2-2\dot{u}_1\dot{u}_2+\dot{u}_2{}^2\right)\right)$$

The potential Energy of the System U is given by equation 10 and is also formed of 3 components: the extension in springs k_1 and k_2, and the bending deformation of the tower with stiffness k_t. It is important to note that u_3 rather u_T is used in the potential energy evaluation as only the deformation due to k_t is evaluated

$$U=\frac{1}{2}k_1u_1{}^2+\frac{1}{2}k_2u_2{}^2+\frac{1}{2}k_tu_3{}^2 \qquad (10)$$

The partial derivatives for the kinetic Energy T in equation 9 are evaluated in equations 11 to 13:

$$\frac{\partial T}{\partial \dot{u}_1}=\frac{1}{4}\left(m_1+m_2\right)\left(\dot{u}_1+\dot{u}_2\right)+\frac{1}{12}m_1\left(\dot{u}_1-\dot{u}_2\right)+m_2\left(\frac{h\dot{u}_3}{L}+\frac{h}{L^2}{}^2\left(\dot{u}_1-\dot{u}_2\right)\right)$$

$$\frac{d}{dt}\frac{\partial T}{\partial \dot{u}_1}=\frac{1}{4}\left(m_1+m_2\right)\left(\ddot{u}_1+\ddot{u}_2\right)+\frac{1}{12}m_1\left(\ddot{u}_1-\ddot{u}_2\right)+m_2\left(\frac{h\ddot{u}_3}{L}+\frac{h}{L^2}{}^2\left(\ddot{u}_1-\ddot{u}_2\right)\right) \qquad (11)$$

$$\frac{\partial T}{\partial \dot{u}_2} = \frac{1}{4}(m_1 + m_2)(\dot{u}_1 + \dot{u}_2) + \frac{1}{12} m_1(\dot{u}_2 - \dot{u}_1) + m_2\left(\frac{-h\dot{u}_3}{L} + \frac{h}{L^2}^2(\dot{u}_2 - \dot{u}_1)\right)$$

$$\frac{d}{dt}\frac{\partial T}{\partial \dot{u}_2} = \frac{1}{4}(m_1 + m_2)(\ddot{u}_1 + \ddot{u}_2) + \frac{1}{12} m_1(\ddot{u}_2 - \ddot{u}_1) + m_2\left(\frac{-h\ddot{u}_3}{L} + \frac{h}{L^2}^2(\ddot{u}_2 - \ddot{u}_1)\right) \quad (12)$$

$$\frac{\partial T}{\partial \dot{u}_3} = m_2\left(\dot{u}_3 + \frac{h}{L}(\dot{u}_1 - \dot{u}_2)\right)$$

$$\frac{d}{dt}\frac{\partial T}{\partial \dot{u}_3} = m_2\left(\ddot{u}_3 + \frac{h}{L}(\ddot{u}_1 - \ddot{u}_2)\right) \quad (13)$$

The equations 11, 12, 13 can be written in Matrix format as shown in equation 14, which is analogous to a mass matrix multiplied by an acceleration matrix

$$= \begin{bmatrix} \frac{m_1}{3} + \frac{m_2}{4} + m_2\frac{h^2}{L^2} & \frac{m_1}{6} + \frac{m_2}{4} - m_2\frac{h^2}{L^2} & m_2\frac{h}{L} \\ \frac{m_1}{6} + \frac{m_2}{4} - m_2\frac{h^2}{L^2} & \frac{m_1}{3} + \frac{m_2}{4} + m_2\frac{h^2}{L^2} & -m_2\frac{h}{L} \\ m_2\frac{h}{L} & -m_2\frac{h}{L} & m_2 \end{bmatrix} \begin{bmatrix} \ddot{u}_1 \\ \ddot{u}_2 \\ \ddot{u}_3 \end{bmatrix} = [M][\ddot{u}] \quad (14)$$

The derivatives of kinetic energy with respect to translation are zero as shown in equation 15

$$\frac{\partial T}{\partial u_1} = \frac{\partial T}{\partial u_2} = \frac{\partial T}{\partial u_3} = 0 \quad (15)$$

The partial derivatives for the potential energy U in the equations are evaluated in equations 16 to 18:

$$\frac{\partial U}{\partial u_1} = k_1 u_1 \quad (16)$$

$$\frac{\partial U}{\partial u_2} = k_2 u_2 \quad (17)$$

$$\frac{\partial U}{\partial u_3} = k_t u_3 \quad (18)$$

Equations 16,17, and 18 can be written in Matrix format as shown in equation 19, which is analogous to a stiffness matrix multiplied by a translation matrix

$$= \begin{bmatrix} k_1 & 0 & 0 \\ 0 & k_2 & 0 \\ 0 & 0 & k_t \end{bmatrix} \begin{bmatrix} u_1 \\ u_2 \\ u_3 \end{bmatrix} = [K][u] \tag{19}$$

The equation of motion $[M][\ddot{u}] + [K][u] = 0$ where M and K are as per equations 14 and 19.

Hence the 3 natural frequencies are the eigen vector solutions which can be solved using any standard mathematics program or even spreadsheet program such as Excel.

$$([K] - \omega^2[M])[u] = 0$$

$$eig[M^{-1}K]$$

(20)

Similarly, if the vibration occurs along the diagonal axes, a third spring k_G a displacement u_G is added to the system as shown in Figure 14. The potential energy of the system previously described in equation 10 such that it can be recalculated as equation 21.

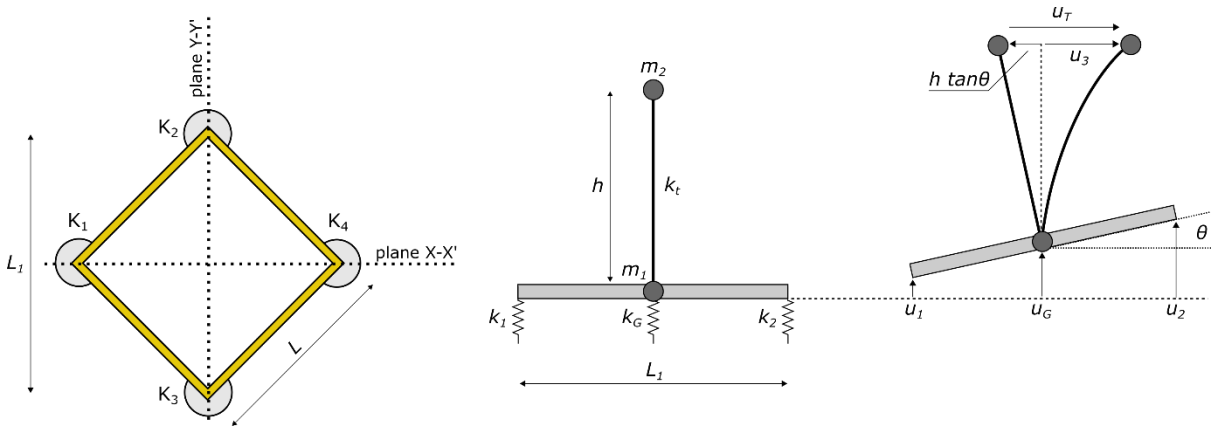

Figure 14 (a): Plan view of the foundation (b) stiffness and mass idealization of the system (c) degrees of freedom of the system

$$U = \frac{1}{2}k_1 u_1^{\,2} + \frac{1}{2}k_2 u_2^{\,2} + \frac{1}{2}k_G u_G^{\,2}\frac{1}{2}k_t u_3^{\,2} \tag{21}$$

As per equation 1, equation 17 can be simplified as

$$U = \frac{1}{2}k_1 u_1^{\,2} + \frac{1}{2}k_2 u_2^{\,2} + \frac{1}{2}k_G\left(\frac{u_1 + u_2}{2}\right)^2 + \frac{1}{2}k_t u_3^{\,2}$$

The partial derivatives for the potential energy U in equation 21 are evaluated in equations 22 to 24

$$\frac{\partial U}{\partial u_1} = k_1 u_1 + \frac{1}{4}k_G(u_1 + u_2) \tag{22}$$

$$\frac{\partial U}{\partial u_2} = k_2 u_2 + \frac{1}{4} k_G \left(u_1 + u_2 \right) \tag{23}$$

$$\frac{\partial U}{\partial u_3} = k_t u_3 \tag{24}$$

Similarly, equation 19 can be adjusted to:

$$= \begin{bmatrix} k_1 + \frac{1}{4} k_G & \frac{1}{4} k_G & 0 \\ \frac{1}{4} k_G & k_2 + \frac{1}{4} k_G & 0 \\ 0 & 0 & k_t \end{bmatrix} \begin{bmatrix} u_1 \\ u_2 \\ u_3 \end{bmatrix} \tag{25}$$

Where

$$k_1 = k_B \tag{26}$$

$$k_1 = k_D \tag{27}$$

$$k_G = k_A + k_C \tag{28}$$

Moreover as $L_1 = \sqrt{2} L$ equation 10 can be changed to

$$= \begin{bmatrix} \frac{m_1}{3} + \frac{m_2}{4} + m_2 \frac{h^2}{2L^2} & \frac{m_1}{6} + \frac{m_2}{4} - m_2 \frac{h^2}{2L^2} & m_2 \frac{h}{\sqrt{2}L} \\ \frac{m_1}{6} + \frac{m_2}{4} - m_2 \frac{h^2}{2L^2} & \frac{m_1}{3} + \frac{m_2}{4} + m_2 \frac{h^2}{2L^2} & -m_2 \frac{h}{\sqrt{2}L} \\ m_2 \frac{h}{\sqrt{2}L} & -m_2 \frac{h}{\sqrt{2}L} & m_2 \end{bmatrix} \begin{bmatrix} \ddot{u}_1 \\ \ddot{u}_2 \\ \ddot{u}_3 \end{bmatrix} \tag{29}$$

The methodology above shows how the fundamental natural frequencies of the system can be computed analytically. As three degrees of freedom are allowed, the modes of vibration will be computed. For the purpose of the problem in hand, only the first mode of vibration which will be either rocking type vibration (Figure 4) or sway-bending (Figure 3) are of main interest.

It is important to highlight that the distribution of accelerating mass can be arbitrarily chosen, and respective Euler-Lagrange equations must be formed. It is convenient to lump the distributed mass at the tip of the cantilever tower. It may be also noted that the provided formulations could be reconstructed in different ways such as splitting the mass of the base to individual masses over the springs, which can be useful if designers have special mass requirements over individual caissons. From the formulations presented, it is clear that different parameters such as the foundation stiffness (k_1 and k_2), geometrical aspect ratio (h/L) are the main parameters affecting the first mode of vibration type of the system. The next section takes a practical example to show the effect of influencing parameters.

4.0 Non-Dimensional study of an example jacket on multiple foundations

For the purpose of this investigation and verifying the obtained mass and stiffness matrices, the jacket of EU funded project Upwind is considered. Essentially, this is four-legged jacket structures supporting a 5 MW wind turbines in deeper waters and the details can be found in [11] and schematically shown in Figure 15. The report also shows how different jacket arrangement and dimensions can be optimized to obtain a satisfactory design. Other necessary information is shown in Table 1 and data pertaining to 5 MW reference wind turbine can be found in [12].

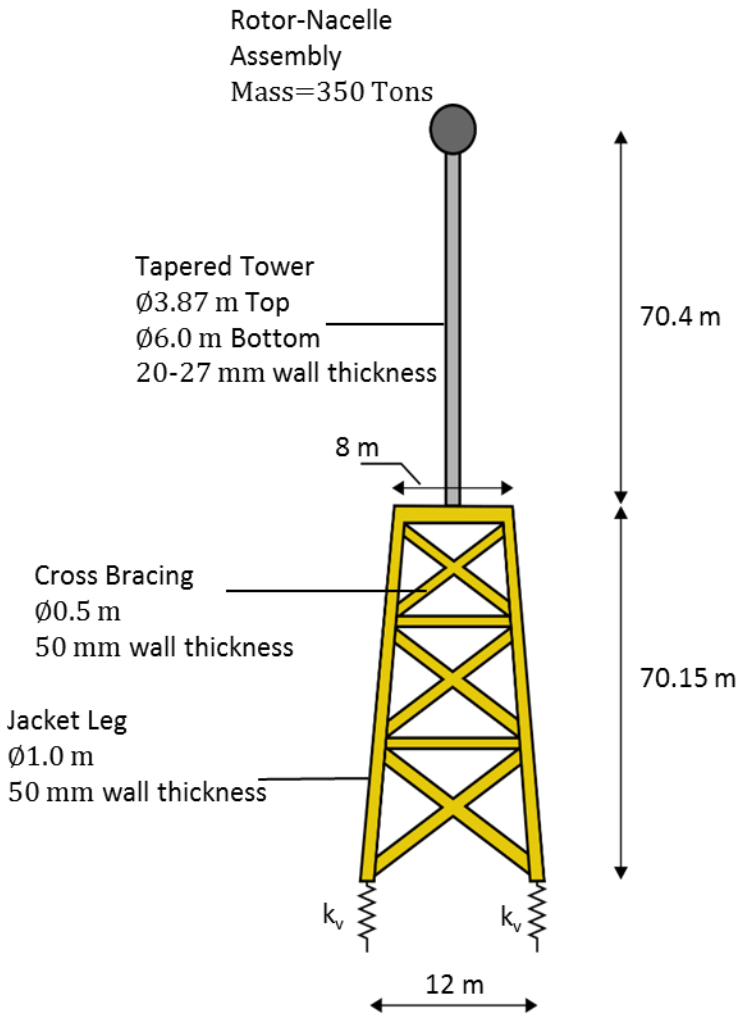

Figure 15: Schematic for example problem and details used for Finite Element Model

Table 1: Jacket and Tower Properties of example problem

Mass of Rotor-Nacelle Assembly	350 tons
Tower Height	70.4 m
Tower Bottom Diameter	6 m (27 mm thick)

Tower Top Diameter	3.87 m (20mm thick)
Jacket Bottom Width	12 m
Jacket Top Width	8 m
Jacket Height	70.15 m
Jacket External Legs	1m (50mm thick)
Jacket Braces	0.5 m (50 mm thick)

The jacket supported system was analysed using the analytical expression derived in Section 3 as well as finite element package SAP2000 for different values of k_v. After obtaining k_t and m_2 from the fixed base finite element model, the mass and stiffness are constructed to obtain equations 14 and 19. Parametric study is conducted to understand the variation of first fundamental frequency (f_0) with increasing vertical stiffness of the springs k_v. Finite element analysis is carried out for the following purposes:

(1) To obtain the fundamental natural frequency using modal analysis to compare with the analytical solution developed in Section 3.
(2) To obtain k_t i.e. stiffness of the tower in the equivalent mechanical model by applying a unit load at the tower tip.
(3) To obtain the equivalent accelerating mass of the superstructure m_2 (jacket, tower, and lumped mass of the RNA). After the fixed-base natural frequency (f_{fb}) is obtained for the full model shown, the accelerating mass m_2 is obtained using $m_2 = \frac{k}{(2\pi f_{fb})^2}$. Alternatively, m_2 can be calculated using the method provided in Appendix 2

It is important to note that the finite element results have been performed through a linear eigenvector analysis on SAP2000. The jacket was constructed using beam elements with moment releases at the ends. The tower consisted of a non-prismatic section with a linear variation of the moment of inertia. As for the accelerating masses, the m_{RNA} was modelled through a lumped mass at the tower top and the program automatically calculates the accelerating mass of the jacket and the tower (superstructure). The foundation supports were modelled using linear springs, this however is an idealization that assumes equivalent axial stiffness of the foundations in both the push-in and pull-out direction. In reality the stiffness is non-isotropic and slight differences in stiffness are expected. Typical deflected mode shape from the software output is shown in Figure 16. Figure 17 shows a comparison between the analytical model and the finite element analysis. The closed form solution provided by Jalbi and Bhattacharya [17] is also used to verify the solutions.

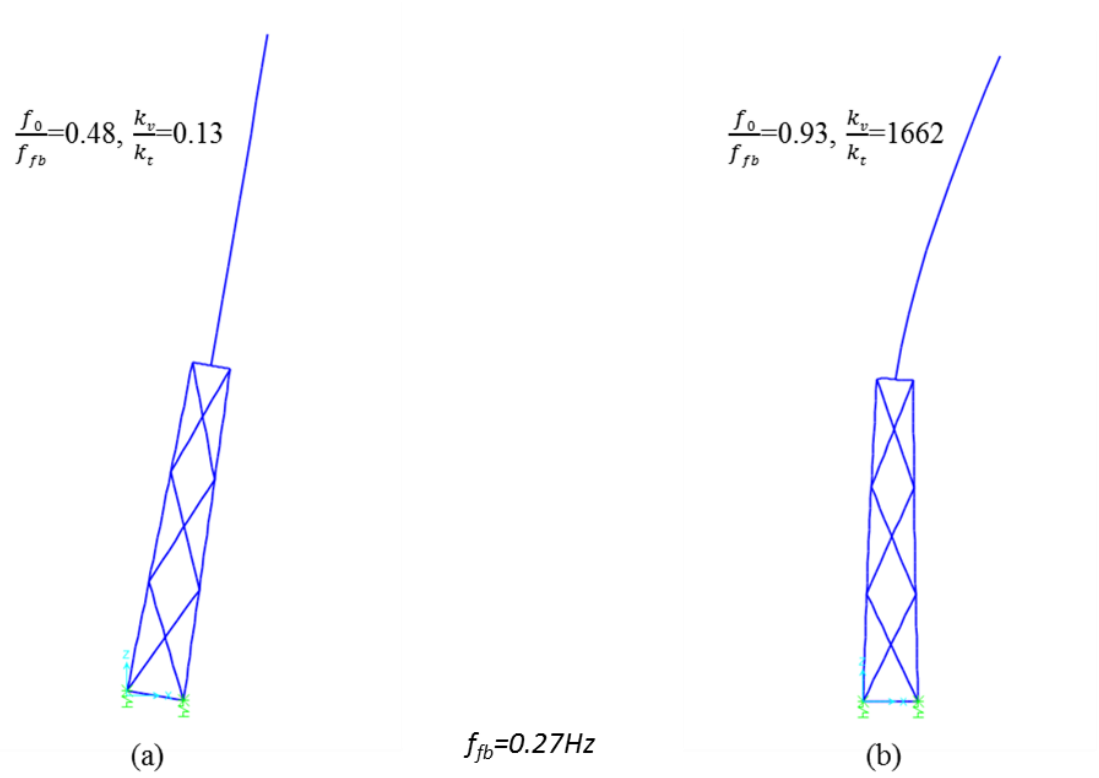

Figure 16: Typical output from Finite Element model showing rocking and sway-bending modes of vibration; (a) Rocking mode of vibration for low k_V values; (b) Sway bending mode for high k_V values.

Note: In a 3D analysis, the natural frequencies in the two orthogonal directions will be almost identical (See Figure 9) if the spring stiffness below each foundation is the same i.e. rocking may occur in fore-aft and side to side vibrations of the structure. It is important to remember that wave loads can change directions making the structure prone to rocking in both directions.

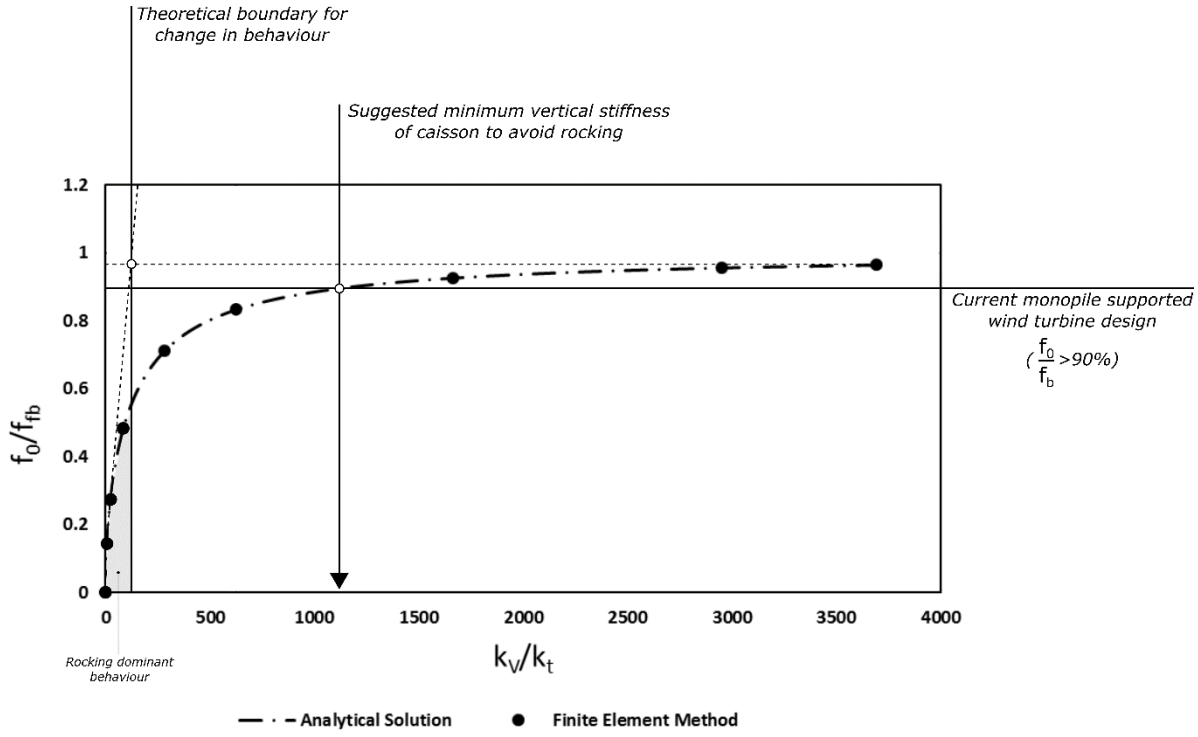

Figure 17: Variation of normalised 1st natural frequency of the system (f_0/f_{fb}) with normalised vertical stiffness of the foundation (k_v/k_t)

Few points may be noted from the graphs.

(1) From Figure 17, it is clear that the analytical solution matches quite well with the finite element analysis which demonstrates that the Euler-Lagrange mass and stiffness matrices obtained are valid. For low vertical stiffness of the foundation, rocking is the dominant vibration mode, see Figure 16(a). Also as the vertical stiffness of the foundation increases, the vibration mode moves to sway-bending and the corresponding 1st natural frequency increase and approaches the fixed base natural frequency.

(2) The parameter dictating whether the system vibrates in a rocking or sway bending mode is the ratio of foundation vertical stiffness (k_V) to superstructure stiffness (k_t). At low foundation stiffness, the structure is more susceptible to rocking, whilst at higher foundation stiffness values sway-bending vibration governs. It is important to note that in the rocking vibration region any change in vertical stiffness results in an abrupt changes in the frequency of the system. Therefore, to avoid rocking an optimization of the relative stiffness may be carried out.

(3) Rocking modes are low frequency and it may interfere with the 1P frequencies of the rotor. Using simple geometrical construction as shown in Figure 17, one can determine the threshold vertical stiffness of the foundation to find the theoretical boundary of two types of vibration mode. Below the threshold vertical stiffness of the foundation, rocking mode of vibration is dominant. Based on the analysis carried out by [9], it is shown that most monopile supported wind turbine are close to the fixed base frequency i.e. value of f_0/f_{fb} close to 0.9. In the absence of monitoring data of jacket supported on shallow foundations, it is suggested to having the vertical stiffness of the foundation such that sway bending mode of vibration governs.

Further analysis has been carried out to study the effect of aspect ratio h/L. For the simplified equivalent model, it is assumed that the stiffness of the superstructure (k_t) does not change with an increasing aspect ratio (by increasing L and keeping h constant). To verify this assumption a study was performed on the model shown in Figure 15 where the bottom width of the jacket was varied and the top width was kept constant at 8 m. The fixed base natural frequency was then recorded for the different cases as shown in Figure 18. It may be noted that the fixed based frequency does not greatly change with increasing length, which means that the analytical method could be used using a constant k_t to study the effect of varying aspect ratio. Figure 19 shows the similar results for different aspect ratio of the jacket. It is clear from the figure that the transition between rocking and sway-bending mode is also affected by the aspect ratio. As expected higher, aspect ratios (lower foundation width) makes the jacket system more susceptible to rocking. Higher h/L value will lead to a lower foundation width and will require higher vertical stiffness of the foundation to engineer towards sway-bending mode.

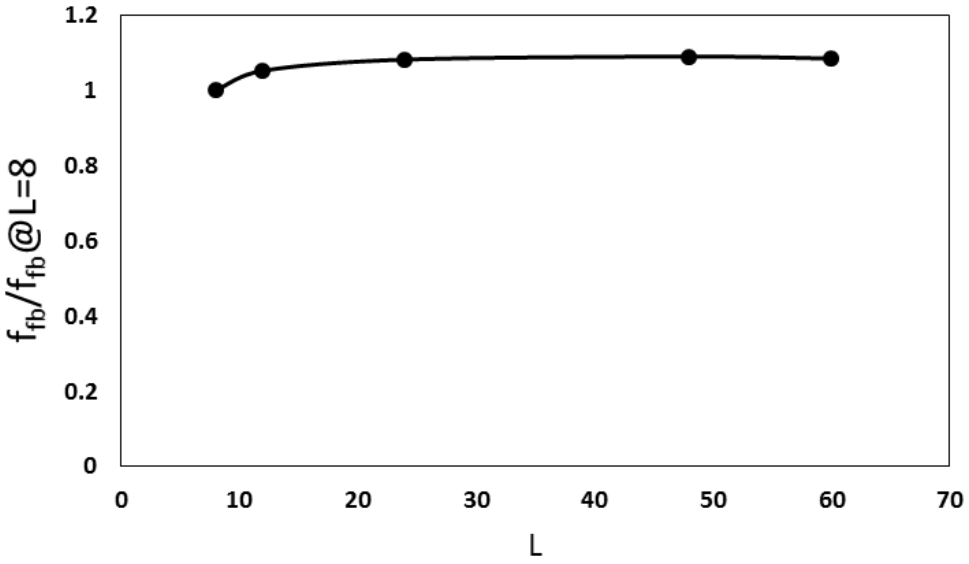

Figure 18: Variation of the fixed base natural frequency with increasing jacket bottom width.

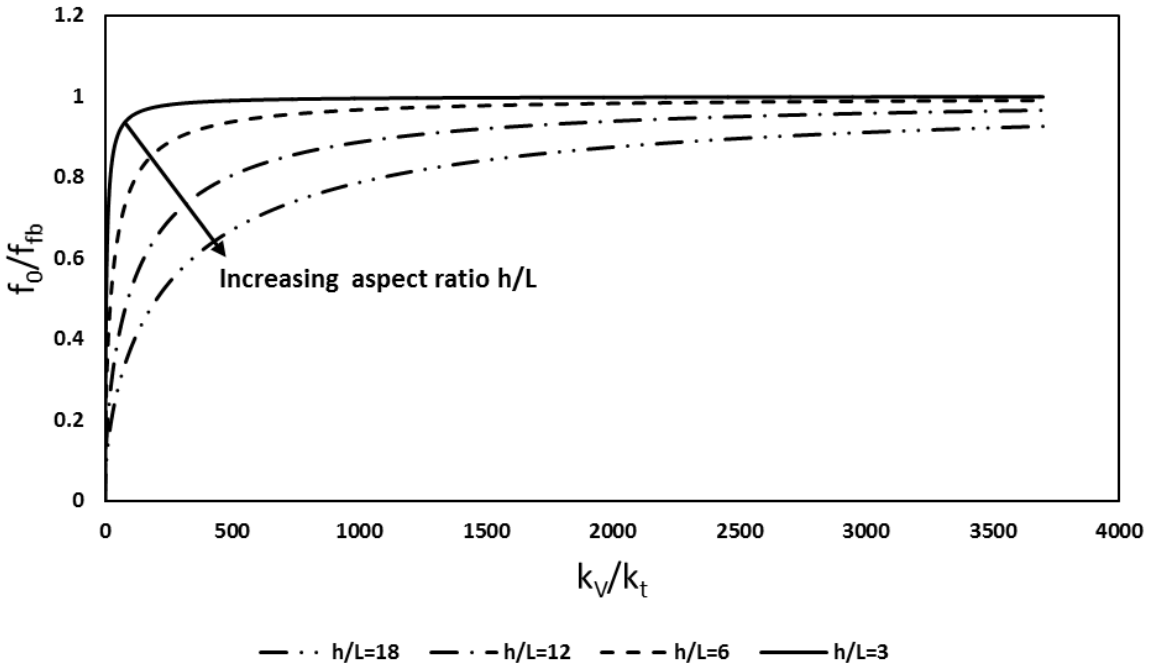

Figure 19: Effect of increasing aspect ratio on the modes of vibration of the system.

It is important to state that though the provided formulation results in 3 natural frequencies, special care should be taken when assessing the 2nd and 3rd frequencies. This is because the value of m_2 (which depends on the accelerating mass of the tower and the jacket), calculated using either substitution from the FEA or using the Appendix 2 is dependent on the function of the first mode of vibration. For preliminary designs, an accurate estimate of the first natural frequency would be sufficient. However, designers willing to calculate subsequent frequencies must derive m_2 using the second and third modes of vibration respectively either by finding it using FEA software as shown above or by changing the mode shape equation in Appendix 2 to the 2nd and 3rd modes of vibration.

It may be also noted that the method presents the first estimate for preliminary design and providing design considerations. For detailed nfa (natural frequency analysis), it is suggested that the mass matrix should also consist of the following

- Mass of tower equipment such as the flanges.
- Mass of working platforms such as such as boat landings, access ladders, resting platforms, and external platforms.
- The mass of the TP, where a methodology to include this is also provided in [17].
- The mass of any heavy grouted connections (if present)
- Environmental conditions such as mass of marine growth and mass of corrosion allowance.

Other environmental factors influencing the stiffness of foundations such as scour should also be considered such as the study shown in [18]

Finally, designers using the provided formulations need to keep in mind current design standards regarding the target frequency for soft-stiff design (which is usually placed between 1P and 3P). For instance, the (DNVGL-ST-0126, 2016) recommends that the natural frequency should have a safety factor margin of 10% on the maximum and minimum rotor speeds (soft-stiff design region). Similarly, the recommended values should also consider the ground material stiffness values when performing

natural frequency analysis (nfa). Typically, the characteristic soil conditions (material safety factor=1) are used for natural frequency analysis.

5.0 Conclusions and Recommendations

Jacket supported on shallow foundations are being considered as foundation solutions for deeper water offshore wind farms. As offshore wind turbines are dynamically sensitive, modes of vibration are an essential design consideration to satisfy the design limit states. This paper shows that depending on the vertical stiffness of the shallow foundation, a jacket structure may exhibit either rocking modes of vibration or sway-bending mode. As rocking modes of vibration are low frequency, these can get tuned with the rotor frequency causing resonance type effects. Drawing an analogy from the well-known *helicopter ground resonance* problem, this study suggests that rocking modes of vibration may be avoided to ensure intended performance in its full design life. Analytical solutions are presented for eigen frequencies of a jacket system and are validated with finite element analysis. A jacket may be engineered towards a no-rocking solution by optimising two parameters: (a) ratio of vertical stiffness of the foundation stiffness to lateral superstructure stiffness; (b) aspect ratio of the jacket-tower geometry. A low value of vertical foundation stiffness values together with a low aspect ratio will promote a rocking mode of vibration. On the other hand, a high vertical stiffness of the foundation with higher aspect ratio (broader base of the tower) will encourage a sway-bending mode. Furthermore, the study shows that the transition from rocking to sway-bending is non-linear and depends not only on the aspect ratio but also on the ratio of vertical stiffness of the foundation and lateral stiffness of jacket-tower configuration. A practical method is shown to choose the vertical stiffness of the foundation to avoid rocking.

Appendix -1: Example configuration of foundations

This section of the appendix shows the centre of mass and centre of stiffness for different foundation arrangements. The centre of stiffness of the foundation "springs" can be defined as the arithmetic mean position of all the spring stiffness values or in other words if the stiffness of all the foundations were to act at a single point. This is done to show that uncoupling between oscillations in orthogonal planes may be permitted in certain situations.

Square foundation arrangement:

Figure A.1 shows the plan view of a square arrangement. The foundations are replaced with linear springs with identical stiffness "k". The base members are assumed to be homogenous with the same density and cross-section, and since they all have the same length, all members have the same mass "m"

Hence, the centre of mass:

$$4m\begin{bmatrix} X \\ Y \end{bmatrix} = m\begin{bmatrix} \frac{L}{2} \\ 0 \end{bmatrix} + m\begin{bmatrix} L \\ \frac{L}{2} \end{bmatrix} + m\begin{bmatrix} \frac{L}{2} \\ L \end{bmatrix} + m\begin{bmatrix} 0 \\ \frac{L}{2} \end{bmatrix} \quad \text{(Eqn A.1)}$$

$$\begin{bmatrix} X \\ Y \end{bmatrix} = \begin{bmatrix} \frac{L}{2} \\ \frac{L}{2} \end{bmatrix} \quad \text{(Eqn A.2)}$$

Centre of Stiffness:

$$4k\begin{bmatrix} X \\ Y \end{bmatrix} = k\begin{bmatrix} 0 \\ 0 \end{bmatrix} + k\begin{bmatrix} 0 \\ 0 \end{bmatrix} + k\begin{bmatrix} L \\ L \end{bmatrix} + k\begin{bmatrix} L \\ L \end{bmatrix} \quad \text{(Eqn A.3)}$$

$$\begin{bmatrix} X \\ Y \end{bmatrix} = \begin{bmatrix} \frac{L}{2} \\ \frac{L}{2} \end{bmatrix} \quad \text{(Eqn A.4)}$$

Judging from Eqns A.2 and A.4, the coordinated of the centre of mass and centre of stiffness coincide which means uncoupling of orthogonal directions is permissible.

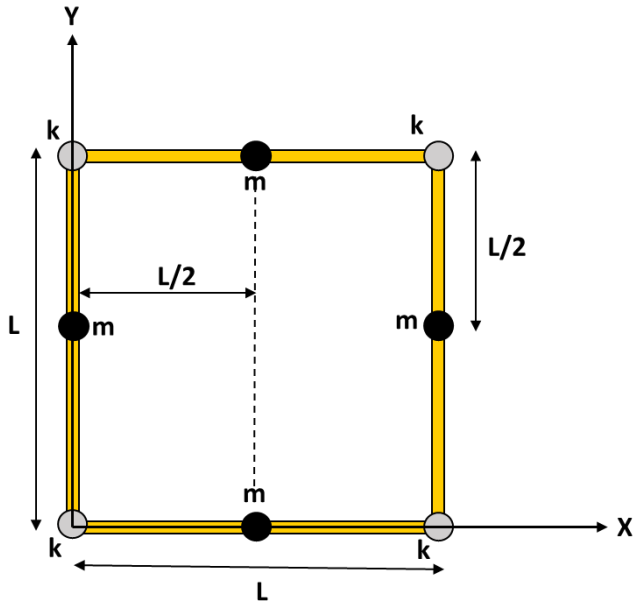

Figure A.1: Plan view of a square foundation arrangement

Symmetric Triangle:

Similarly, for a symmetric triangle as shown in schematic Figure A.2, the centre of mass may be computed as:

$$3m\begin{bmatrix} X \\ Y \end{bmatrix} = m\begin{bmatrix} \frac{L}{2} \\ 0 \end{bmatrix} + m\begin{bmatrix} \frac{L}{4} \\ \frac{\sqrt{3}L}{4} \end{bmatrix} + m\begin{bmatrix} \frac{3L}{4} \\ \frac{\sqrt{3}L}{4} \end{bmatrix} \quad \text{(Eqn A.5)}$$

$$\begin{bmatrix} X \\ Y \end{bmatrix} = \begin{bmatrix} \frac{L}{2} \\ \frac{\sqrt{3}L}{6} \end{bmatrix} \quad \text{(Eqn A.6)}$$

And the centre of stiffness as shown in equation A.7

$$3k\begin{bmatrix} X \\ Y \end{bmatrix} = k\begin{bmatrix} 0 \\ 0 \end{bmatrix} + k\begin{bmatrix} L \\ 0 \end{bmatrix} + k\begin{bmatrix} \frac{L}{2} \\ \frac{\sqrt{3}L}{2} \end{bmatrix} \quad \text{(Eqn A.7)}$$

$$\begin{bmatrix} X \\ Y \end{bmatrix} = \begin{bmatrix} \frac{L}{2} \\ \frac{\sqrt{3}L}{6} \end{bmatrix} \quad \text{(Eqn A.8)}$$

In a similar manner to the square foundations, uncoupling may be performed on symmetric triangles with identical foundations.

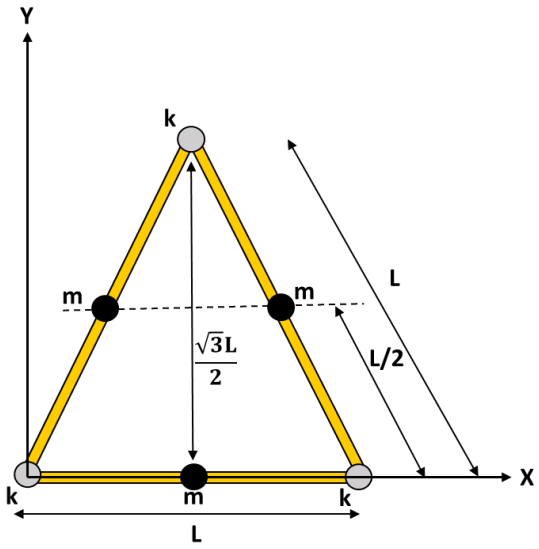

Figure A.2: Plan view of a symmetric triangle foundation arrangement

Asymmetric Triangles

Consider the asymmetric triangle shown in Figure A.3. Retaining the assumption that the members of the foundation have the same density and cross-section, the mass of the horizontal member is $\sqrt{2}$ times the mass of other members due to its length.

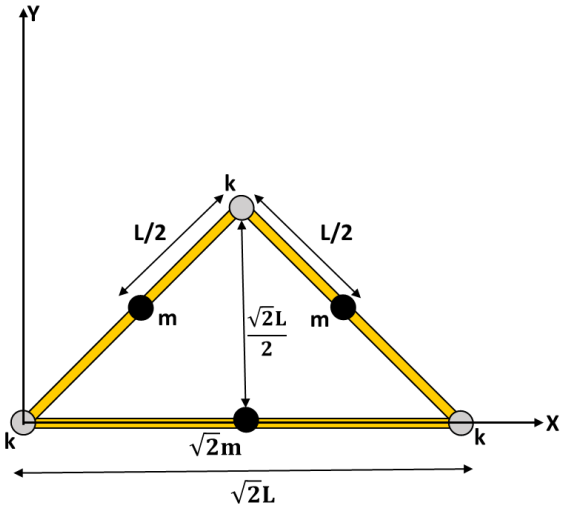

Figure A.3 Plan view of an asymmetric triangle foundation arrangement

Centre of mass:

$$\left(2+\sqrt{2}\right)\mathrm{m}\begin{bmatrix}\mathrm{X}\\ \mathrm{Y}\end{bmatrix}=\sqrt{2}\mathrm{m}\begin{bmatrix}\frac{\sqrt{2}\mathrm{L}}{2}\\ 0\end{bmatrix}+\mathrm{m}\begin{bmatrix}\frac{\sqrt{2}\mathrm{L}}{4}\\ \frac{\sqrt{2}\mathrm{L}}{4}\end{bmatrix}+\mathrm{m}\begin{bmatrix}\frac{3\sqrt{2}\mathrm{L}}{4}\\ \frac{\sqrt{2}\mathrm{L}}{4}\end{bmatrix} \qquad \text{(Eqn A.9)}$$

$$\begin{bmatrix} X \\ Y \end{bmatrix} = \begin{bmatrix} \frac{\sqrt{2}L}{2} \\ \frac{\left(-1+\sqrt{2}\right)L}{2} \end{bmatrix} \qquad \text{(Eqn A.10)}$$

Similarly, the centre of stiffness is

$$3k\begin{bmatrix} X \\ Y \end{bmatrix} = k\begin{bmatrix} 0 \\ 0 \end{bmatrix} + k\begin{bmatrix} \sqrt{2}L \\ 0 \end{bmatrix} + k\begin{bmatrix} \frac{\sqrt{2}L}{2} \\ \frac{\sqrt{2}L}{2} \end{bmatrix} \qquad \text{(Eqn A.11)}$$

$$\begin{bmatrix} X \\ Y \end{bmatrix} = \begin{bmatrix} \frac{\sqrt{2}L}{2} \\ \frac{\sqrt{2}L}{6} \end{bmatrix} \qquad \text{(Eqn A.12)}$$

Judging from Eqns A.10 and A.12, vibrations across orthogonal planes cannot be assessed independently and a 3D Lagrange formulation is required. If however, the mass of the horizontal member is m rather than $\sqrt{2}$ m (Due to a smaller cross section for instance) the centre of mass equation becomes as follows :

$$3m\begin{bmatrix} X \\ Y \end{bmatrix} = m\begin{bmatrix} \frac{\sqrt{2}L}{2} \\ 0 \end{bmatrix} + m\begin{bmatrix} \frac{\sqrt{2}L}{4} \\ \frac{\sqrt{2}L}{4} \end{bmatrix} + m\begin{bmatrix} \frac{3\sqrt{2}L}{4} \\ \frac{\sqrt{2}L}{4} \end{bmatrix} \qquad \text{(Eq A.13)}$$

$$\begin{bmatrix} X \\ Y \end{bmatrix} = \begin{bmatrix} \frac{\sqrt{2}L}{2} \\ \frac{\sqrt{2}L}{6} \end{bmatrix} \qquad \text{(Eq A.14)}$$

Now judging from equations A.14 with A.12, a match is observed and thus decoupling may occur even with an asymmetrical arrangement.

Appendix -2: Calculation of lumped mass m_2

At this stage, designers can estimate the distributed mass of the jacket and tower in kg/m as shown in Figure A.4. The first step in obtaining m_2 is to obtain the equivalent distributed mass of the tower and jacket system $m_{eq.}$ The Kinetic Energy of the system is calculated as per Eq A.15

$$KE=\int m(z)\varphi^2 dz \qquad \text{(Eq A.15)}$$

Where m(z) and ϕ are the mass and eigen mode function of a continuous cantilever system. Equating the Kinetic energy of the tower-jacket system with the equivalent beam

$$\int m(z)\varphi^2 dz=\int m_{eq}\varphi^2 dz$$

Further simplification leads to

$$m_{eq}=\frac{\int m(z)\varphi_1{}^2 dz}{\int \varphi_1{}^2 dz}=\frac{\sum_{i=1}^{n} m_i \int_{z(i-1)}^{z(i)} \varphi_1{}^2 dz}{\int_0^{z(i)} \varphi_1{}^2 dz}=\frac{m_J \int_0^{h_J} \varphi_1{}^2 dz+m_T \int_{h_J}^{h_J+h_T} \varphi_1{}^2 dz}{\int_0^{h_T+h_J} \varphi_1{}^2 dz} \qquad \text{(Eq A.16)}$$

The value of the integral of the square of the first mode function can be evaluated using Eq A.17

$$\int \varphi_1{}^2 dz=z+\frac{1-\beta_1{}^2}{\frac{4\lambda_1}{L}}\sin\frac{2\lambda_1}{L}z-\frac{\beta_1}{\frac{2\lambda_1}{L}}\cos\frac{2\lambda_1}{L}z+\frac{1+\beta_1{}^2}{\frac{4\lambda_1}{L}}\sinh\frac{2\lambda_1}{L}z+\frac{\beta_1{}^2}{\frac{2\lambda_1}{L}}\cosh\frac{2\lambda_1}{L}z-\frac{2\beta_1}{\frac{\lambda_1}{L}}\sin\frac{\lambda_1}{L}z\times\sinh\frac{\lambda_1}{L}z-$$

$$\frac{1+\beta_1{}^2}{\frac{\lambda_1}{L}}\sin\frac{\lambda_1}{L}z\times\cosh\frac{\lambda_1}{L}z-\frac{1-\beta_1{}^2}{\frac{\lambda_1}{L}}\cos\frac{\lambda_1}{L}z\times\sinh\frac{\lambda_1}{L}z$$

(Eq A.17)

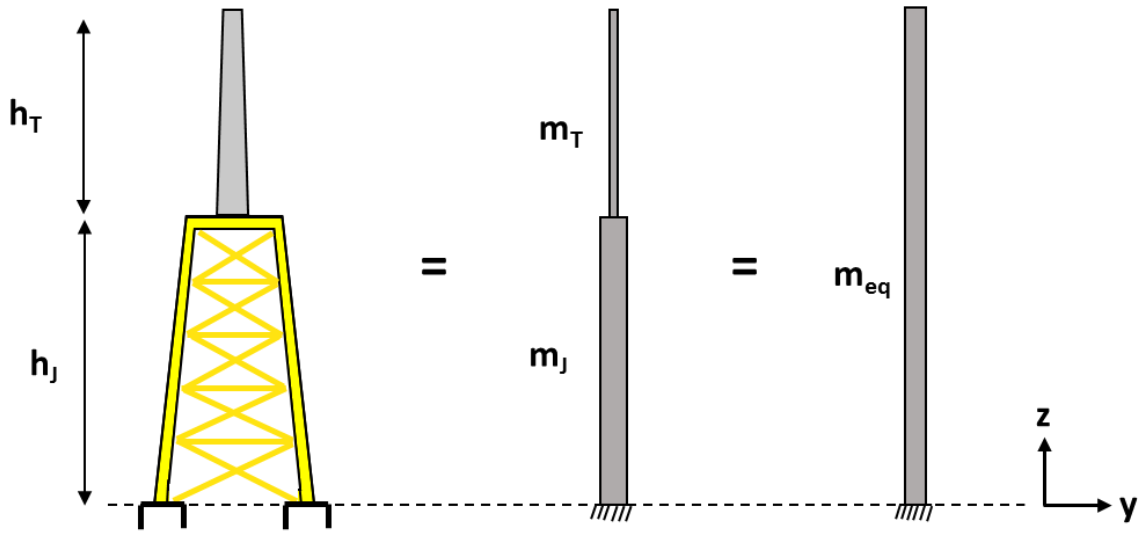

Figure A.4: Equivalent distributed mass of a jacket

Such that

$$L=h_J+h_T$$

And

Where λ_1 and β_1 dimensionless natural frequency parameters of an Euler-Bernoulli cantilever beam

$\lambda = 1.8751$ and

$$\beta_1 = -\frac{\cos\lambda_1+\cosh\lambda_1}{\sin\lambda_1+\sinh\lambda_1}$$

The second step is to obtain the equivalent lumped mass at the tip of the tower in kg

Which is calculated as

$$m_2=\varepsilon\left(m_{eq}h_{total}\right)+M_{RNA}$$

Where ε has been derived to be ε=0.243

It may be reminded that this method is applicable to the first mode of vibration for higher mode of vibrations the second mode ϕ_2 should be used rather than ϕ_1

Appendix -3: Computation of vertical stiffness for shallow foundations k_v

Table A.1 provides guidance on how to compute for shallow embedded foundations. It must be mentioned that the method presented in this paper assumes a "linear" response of the foundations to obtain the natural frequencies

Table A.1: Guidance on the selection of vertical

Shallow foundations		
Reference	Applicability	Vertical stiffness
(Gazetas, 1991) [23]	For *rigid* shallow embedded foundations in homogeneous ground profiles	$k_v = \frac{2.01 G_s D_C}{(1-\upsilon_s)} \left(1.02+0.1\frac{L_C}{D_C}\right)\left(1+0.51\left(\frac{L_C}{D_C}\right)^{\frac{2}{3}}\right)$
(Wolf & Deeks, 2004)[24]	For *rigid* shallow embedded foundations in homogenous ground profiles	$k_v = \frac{2 G_s D_C}{(1-\upsilon_s)} \left(1+1.08\frac{L_C}{D_C}\right)$
(Doherty, et al., 2005) [25]	For *rigid* shallow caissons in homogenous, parabolic, and linear ground profiles	Solution for vertical stiffness of caissons provided in tabular format and is dependent on relative soil to pile stiffness, embedment ratio, and ground profile stiffness variation with depth
(Skau, et al., 2018) [26]	For *flexible* shallow suction caissons. Dependent on finite element soil model for the extraction of the macro-element model	Adjusted the macro-element model provided in [27] (which assumes rigid behaviour) where the bending of the caisson lid in the vertical direction inherently reduces the stiffness of the foundation in addition to changing the volume of the soil plug, i.e. changing the stress state of the soil which also reduces the stiffness. This has also been observed by site measurements shown in [28]

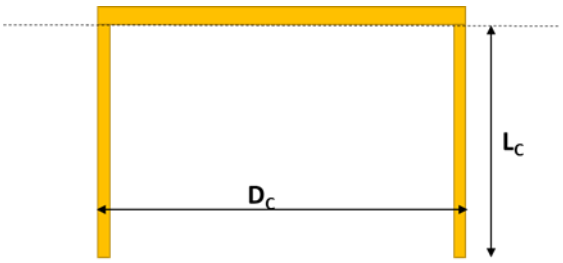

Acknowledgements: The authors would like to thank Hassan A Moharam for help in the analysis.

References

[1] 4C Offshore Limited. Global offshore wind farms database. In: 4COffshore.com web page. ⟨http://www.4coffshore.com/windfarms/⟩; 2015 [accessed 12.10.17].

[2] 4C Offshore Limited. Offshore wind turbine database. In: 4COffshore.com web page. ⟨http://www.4coffshore.com/windfarms/turbines.aspx⟩; 2015 [accessed 12.10.17]

[3] Adhikari, S. & Bhattacharya, S., 2011. Vibrations of wind turbines considering soil-structure interaction. Wind Struct, 14(2), pp. 85-112.

[4] Adhikari, S. & Bhattacharya, S., 2012. Dynamic Analysis of wind turbine towers on flexible foundations. Shock Vib, 19(1), pp. 37-56.

[5] Alexander, N. A., 2010. Estimating the nonlinear resonant frequency of a single pile in nonlinear soil. Sound and Vibration, Issue 329, pp. 1137-1153.

[6] Arany, L., Bhattacharya, S., Macdonald, J. H. & John Hogan, S., 2016. Closed form solution of Eigen frequency of monopile supported offshore wind turbines in deeper water incorporating stiffness of substructure and ssi. Soil Dynamics and Earthquake Engineering, Volume 83, pp. 18-32.

[7] Bhattacharya, S., Adhikari, S. & Alexander, N. A., 2009. A simplified method for unified buckling and free vibration analysis of pile-supported structures in seismically liquefiable soils. Soil Dynamics and Earthquake Engineering, 29(8), pp. 1220-1235.

[8] Bhattacharya, S., Cox, J. A., Lombardi, D. & Muir Wood, D., 2011. Dynamics of offshore wind turbines supported on two foundations. Geotechnical Engineering, pp. 159-169.

[9] Bhattacharya, S., Nikitas, G., Arany, L. & Nikitas, N., 2017. Soil-Structure Interactions for Offshore Wind Turbines. Engineering and Technology.

[10] Bhattacharya, S., Nikitas, N., Garnsey, J., Alexander, N.A., Cox, J., Lombardi, D., Wood, D.M. and Nash, D.F., 2013. Observed dynamic soil–structure interaction in scale testing of offshore wind turbine foundations. *Soil Dynamics and Earthquake Engineering*, *54*, pp.47-60.

[11] De Vries, W., Vemula, N.K., Passon, P., Fischer, T., Kaufer, D., Matha, D., Schmidt, B. and Vorpahl, F., 2011. Support structure concepts for deep water sites. *Delft University of Technology, Delft, The Netherlands, Technical Report No. UpWind Final Report WP4*, *2*, pp.167-187.

[12] Jonkman, J., Butterfield, S., Musial, W. and Scott, G., 2009. *Definition of a 5-MW reference wind turbine for offshore system development* (No. NREL/TP-500-38060). National Renewable Energy Laboratory (NREL), Golden, CO

[13] Squorch, 2006*, Ground Resonance:Rear View*, [accessed 1.10.17], https://www.youtube.com/watch?v=D2tHA7KmRME

[14] Wei, K., Myers, A.T. and Arwade, S.R., 2017. Dynamic effects in the response of offshore wind turbines supported by jackets under wave loading. *Engineering Structures*, *142*, pp.36-45.

[15] Abhinav, K.A. and Saha, N., 2015. Coupled hydrodynamic and geotechnical analysis of jacket offshore wind turbine. *Soil Dynamics and Earthquake Engineering*, *73*, pp.66-79.

[16] Abhinav, K.A. and Saha, N., 2018. Nonlinear dynamical behaviour of jacket supported offshore wind turbines in loose sand. *Marine Structures*, *57*, pp.133-151.

[17] Jalbi, S. and Bhattacharya, S., 2018. Closed form solution for the first natural frequency of offshore wind turbine jackets supported on multiple foundations incorporating soil-structure interaction. *Soil Dynamics and Earthquake Engineering*, *113*, pp.593-613.

[18] Fazeres-Ferradosa, T., Taveira-Pinto, F., Romão, X., Vanem, E., Reis, M.T. and das Neves, L., 2018. Probabilistic design and reliability analysis of scour protections for offshore windfarms. *Engineering Failure Analysis*, *91*, pp.291-305.

[19] Shi, W., Park, H.C., Chung, C.W., Shin, H.K., Kim, S.H., Lee, S.S. and Kim, C.W., 2015. Soil-structure interaction on the response of jacket-type offshore wind turbine. International Journal of Precision Engineering and Manufacturing-Green Technology, 2(2), pp.139-148.

[20] Mostafa, Y.E. and El Naggar, M.H., 2004. Response of fixed offshore platforms to wave and current loading including soil–structure interaction. Soil Dynamics and Earthquake Engineering, 24(4), pp.357-368.

[21] Elshafey, A.A., Haddara, M.R. and Marzouk, H., 2009. Dynamic response of offshore jacket structures under random loads. Marine Structures, 22(3), pp.504-521.

[22] Dong, W., Moan, T. and Gao, Z., 2011. Long-term fatigue analysis of multi-planar tubular joints for jacket-type offshore wind turbine in time domain. Engineering Structures, 33(6), pp.2002-2014.

[23] Gazetas, G., 1991. Formulas and charts for impedances of surface and embedded foundations. *Journal of geotechnical engineering,* 117(9), pp. 1363-1381.

[24] Wolf, J. P. & Deeks, A. J., 2004. *Foundation vibration analysis: A strength of materials approach.* Oxford: Butterworth-Heinemann.

[25] Doherty, J. P., Houlsby, G. T. & Deeks, A. J., 2005. Stiffness of flexible caisson foundations embedded in nonhomogeneous elastic soil. *Journal of geotechnical and geoenvironmental engineering,* 131(12), pp. 1498-1508.

[26] Skau, K.S., Jostad, H.P., Eiksund, G. and Sturm, H., 2019. Modelling of soil-structure-interaction for flexible caissons for offshore wind turbines. *Ocean Engineering*, *171*, pp.273-285.

[27] Skau, K.S., Grimstad, G., Page, A.M., Eiksund, G.R. and Jostad, H.P., 2018. A macro-element for integrated time domain analyses representing bucket foundations for offshore wind turbines. *Marine Structures*, *59*, pp.158-178

[28] Shonberg, A., Harte, M., Aghakouchak, A., Pachecco, M., Cameron, S.D., Lingaard, M., 2017. Suction bucket jackets for offshore wind turbines: applications from in situ observations. In: Proceedings of the 19th International Conferance on Soil Mechanics and Geotechnical Engineering. Soul.